



# Non-Equilibrium Plasma Jet at Atmospheric Pressure Powered by Tesla Coil

Research Article

Gamal M. Elaragi

Plasma Physics and Nuclear Fusion Department, N.R.C. Egyptian Atomic Energy, Cairo, Egypt  
elaragi@gmail.com

**Abstract.** The aim of this work presents the characterization of a plasma jet powered by Tesla coil. Tesla coil can be used for generation cold plasma from *Dielectric Barrier Discharge* (DBD). Tesla coil has been designed and constructed at Egyptian Atomic Energy Authority for multipurpose. The electrical characteristic of non-equilibrium plasma jet using rare gases (argon and helium) at atmospheric pressure has been studied. An atmospheric-pressure cold plasma jet generated by Tesla coil in a single-electrode configuration is characterized based on optical and electrical measurements.

**Keywords.** Cold plasma; Plasma jet; DBD; Non-equilibrium plasma; Tesla coil

**PACS.** 52.70.Kz; 52.70.-m; 52.75.-d; 52.80.-s; 84.30.Jc

**Received:** April 11, 2019

**Accepted:** April 20, 2019

Copyright © 2019 Gamal M. Elaragi. *This is an open access article distributed under the Creative Commons Attribution License, which permits unrestricted use, distribution, and reproduction in any medium, provided the original work is properly cited.*

## 1. Introduction

Non-equilibrium atmospheric pressure plasmas have been attracting increasing attention due to their diversified applications in materials processing and biomedical engineering. The atmospheric-pressure plasma jets are especially favorable because they are generated in the open air rather than in a confined discharge gap, which can be used in direct treatment without limitation on the size of treated objects. Characterization of cold plasma jet is very important tool to have a better control on the plasma applications.

The Tesla coil is an electrical resonant transformer circuit designed by inventor Nikola Tesla around 1891 as a power supply. It is used to produce high-voltage, low-current, and high frequency alternating-current electricity. Tesla experimented with a number of different configurations consisting of two coupled resonant electric circuits. By adjusting the coil and

the capacitor Tesla found he could take advantage of the resonance set up between the two to achieve even higher frequencies. In Tesla's coil transformer the capacitor, upon break-down of a short spark gap, became connected to a coil of a few turns, forming a resonant circuit with the frequency of oscillation, usually 20-100 kHz, determined by the capacitance of the capacitor and the inductance of the coil.

The spark gap is set up so that its breakdown occurs at a voltage somewhat less than the peak output voltage of the transformer in order to maximize the voltage across the capacitor. The sudden current through the spark gap causes the primary resonant circuit to ring at its resonant frequency. The ringing primary winding magnetically couples energy into the secondary over several RF cycles, until all of the energy that was originally in the primary has been transferred to the secondary. Ideally, the gap would then stop conducting (quench), trapping all of the energy into the oscillating secondary circuit. Usually the gap reignites, and energy in the secondary transfers back to the primary circuit over several more RF cycles. Cycling of energy may repeat for several times until the spark gap finally quenches. Once the gap stops conducting, the transformer begins recharging the capacitor. Depending on the breakdown voltage of the spark gap, it may fire many times during a mains AC cycle.

## 2. Experimental Set-Up

The experimental system is composed of: high-voltage, low-current, and high frequency alternating-current electricity; plasma jet generator and gas flow circuit.

Testing Tesla coil can be easily done by two methods. Number one is to visually see the sparks created by the secondary coil by bringing any metal object near the open end. This will cause a small streak of lighting to the metal. The second would be bringing any light bulb near the secondary coil. The field created by the secondary interacts with the gas present inside the light bulb, which ionizes the gas present inside them. This causes the electrons to excite and when they return to their normal state they emit light. Thus the light bulb will be laminated just by being brought near to the secondary coil. The lamination will depend on the distance and the output of the circuit.

A set of experiments were carried out to determine the output of the device. Different kind of tests was done to find the maximum range, Voltage and current outputs, spark lengths etc. The first experiment was to check the output range of the device with the variation of input voltage. For this experiment, the variable voltage source is kept at a constant voltage and then the fluorescent lamp light is brought near the secondary coil. As the light is brought near it starts to glow. Thus starting from zero distance it is moved farther away parallel to the ground. As the distance increases the amount of brightness decreases. Thus the distance is proportional to the output of the coil. Then after a certain distance the fluorescent lamp will stop laminating. This point was noted and is the maximum range for that specific voltage input. This experiment is repeated with different set of input voltages. The results show us a direct relation between the areas of the field is directly proportional to the input voltage being fed to the circuit. The photograph of experiment can be shown in Figure 1 and the circuit of tesla coil already presented in details in a previous article [10].



**Figure 1.** The photograph of experimental setup

The plasma source is a single electrode plasma jet suitable for the treatment of different biological materials. Plasma jet can be used a simple medical syringe whose piston was fitted with a metallic needle. The gas (helium, argon), which is the medium of the discharge is introduced through the syringe piston. The gas flows were in the range 1-4 L/min. The discharge takes place between the metallic needle top and a metallic ring fit on the outer surface of the syringe. The applied voltage is measured by using the high-voltage probe and discharge current was measured using current monitor.

### 3. Results and Discussion

Noble gases such as helium and argon have been used as operating gases, usually at flow rates in the 1-10 L/m range. Admixtures of air or oxygen can be added to these background gases. Depending on the power applied, the gas type, and flow rate, stable plasma plumes with lengths up to several centimeters have routinely been generated. Because the plasmas generated by non-equilibrium atmospheric pressure plasma jets (N-APPJs) are launched in air, they provide very interesting reactive chemistry that can be exploited in various plasma processing applications. Reactive oxygen species (ROS), such as O, OH, and O<sub>2</sub>, and reactive nitrogen species (RNS), such as NO and NO<sub>2</sub>, are abundantly produced. These reactive species have important biological implications such as the inactivation of pathogenic bacteria and the destruction of cancer cells [13–18].

#### 3.1 Electrical Characteristics

The voltage-current waveforms of the plasma jet were measured at constant applied voltage and different gases. Figure 2 shows one of the typical voltage-current shows a typical waveform of dielectric barrier discharge-current waveforms of argon and apparent power was calculated

from multiplying voltage by current. In the traced waveform, we have seen current is more fluctuated than voltage with respect to time. Figure 3 indicates a typical power waveform of it. Figure 4 shows one of the typical voltage-current shows a typical waveform of discharge-current of helium and Figure 5 shows the power waveform of it. The discharge current is caused by charge accumulation on the dielectric surface. This surface charge creates an electric potential that opposes the applied voltage and, as a result, limits the discharge current and prevents the glow-to-arc transition. The initial current and power signals of argon contain series of short consecutive peaks resembling beats i.e. the DBD current indicates that the plasma operates in a filamentary operation mode. The electron density in argon plasma, given by  $n_e = j/(E\mu_e e)$  is estimated to be about  $\approx 2.5 \times 10^{12} \text{ cm}^{-3}$  and for helium  $\approx 9 \times 10^{12} \text{ cm}^{-3}$ . Here,  $e$  is the electron charge,  $E$  the electric field,  $j$  the current density, and  $\mu_e$  the electron mobility.

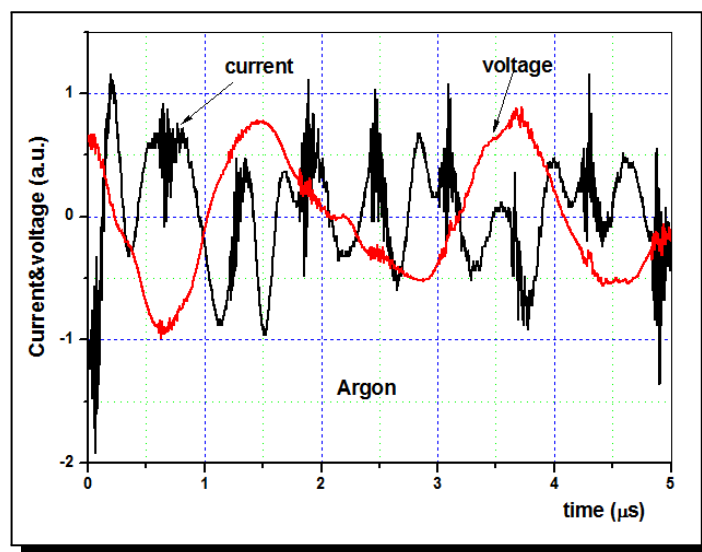


Figure 2. Typical voltage-current waveforms of argon plasma jet

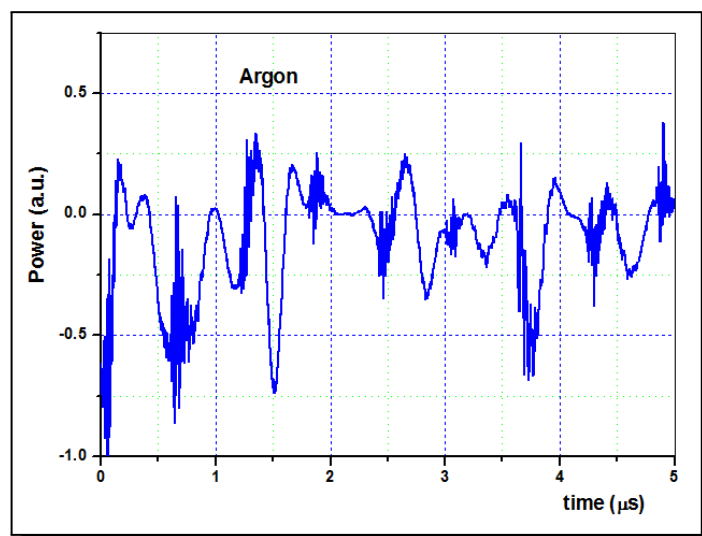


Figure 3. One of the typical power waveform of argon plasma jet

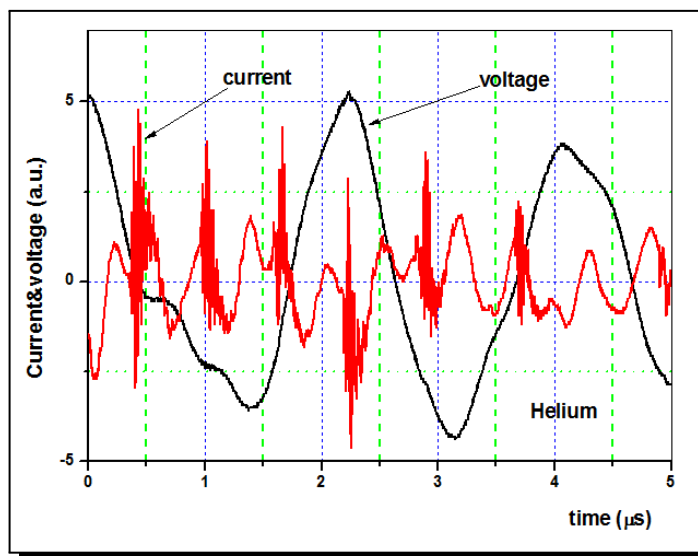


Figure 4. Typical voltage-current waveforms of helium plasma jet

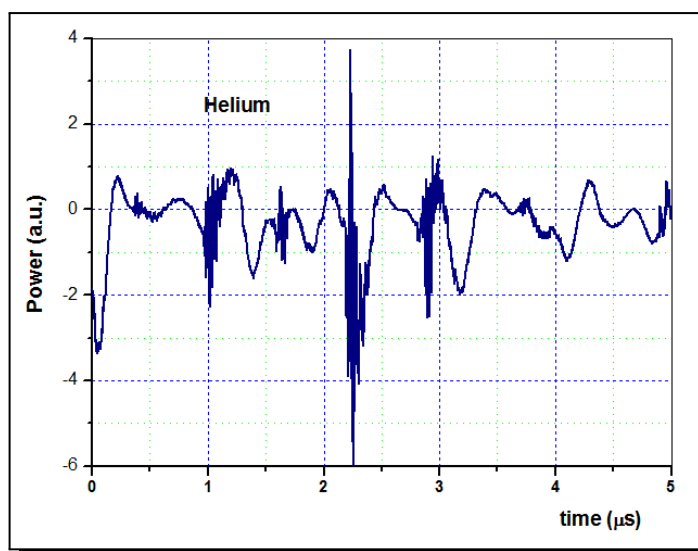
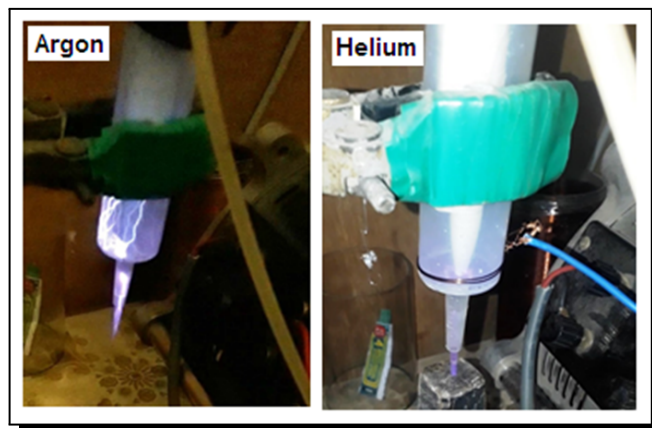


Figure 5. Typical power waveform of helium plasma jet

### 3.2 Optical Characteristics

The working gas was fed into the syringe with a flow rate controlled by a flow meter. During the experiments, the gas flow was varied in the range of 1-4 L/min for both argon and helium, whereas an ac high-voltage signal was applied to the electrode. The maximal length of the argon plume was around 1.5 cm, whereas the extension of the helium plume approached 3 cm. Images of a typical plasma jet created in helium and argon gases at constant applied voltage and different flow rates are taken to get the optimum condition of plasma jet operation for the two gases. Figure 6 shows images of plasma jet for argon and helium at 2.5 L/min and 3.5 L/min respectively.



**Figure 6.** Images of a plasma jet arising with Floating Electrode Dielectric Barrier Discharge (FE-DBD)

In argon plasma the spikes were associated with the formation of micro-discharges (filaments), which were distributed inside the discharge area. These spikes were not detected when helium gas was used because, in this case, the discharge inside the syringe was quite uniform without filaments. The helium plasma was ignited by Tesla coil and the discharge filled the entire volume of the syringe. Inside the syringe, the argon discharge operated in filamentary mode with tiny micro-discharges starting at the high-voltage electrode and terminating on the glass wall.

It was found that the plasma jet length increase with the increase of applied voltage until reached maximum value then it saturates or slightly decreases. When the applied voltage increases, more energetic species are created and their pronounced energy allows them to penetrate deeper into the surrounding air, leading to the formation of an extended plasma jet.

For the characterization of the plasma jet, a dielectric probe is used to measure the jet current. This probe is made of a small copper plate covered by a dielectric sheet. The schematic of this dielectric probe is shown in Figure 7.

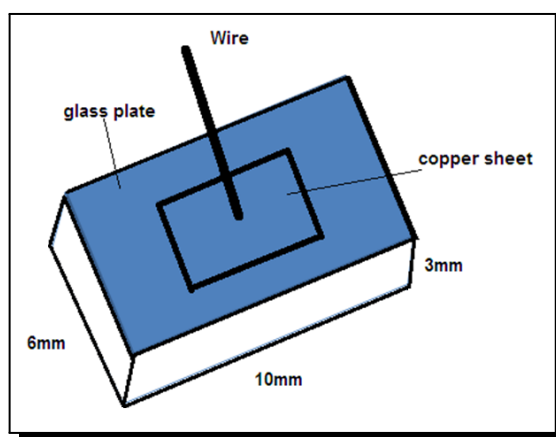


**Figure 7.** Schematic of the dielectric probe

The probe diagnostic method is direct contact method and there is always perturbation in the plasma due to the probe [11]. To understand plasma jet spreading in the ambient atmosphere,

the study of the plasma plume velocity is important. The dielectric probe was placed at different distances ( $Z$ ) from the tip of the tube along the jet axis, and the plume current was measured at those distances. The plume current through dielectric probe were measured different distances along the jet axis. I was found that the time delay for Helium is shorter than the time delay for Argon. The peak current of plasma plume at different probe's distance on the jet's axis for helium and argon plasma jet are shown in Figure 8. It was noticed that, the peak current decreases with the increase in probe's distance along the jet's. The decrease of peak current with the increase in probe's distances along the jet's axis shows that, there is a low density plasma channel behind the head of the plasma bullet [11].

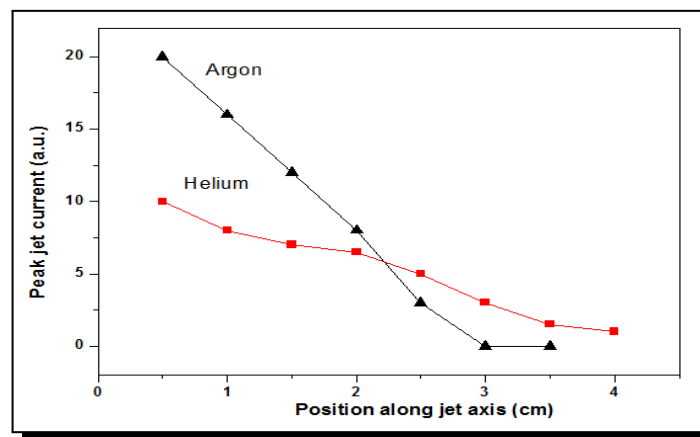


**Figure 8.** The peak jet current at different probe's position along the jet's axis for Helium jet at 4L/min flow rate and (b) Argon jet at 2.5 L/min flow rate

The plasma plume velocity (bullet) was measured at different axial distance along the jet's axis. Figure 9 shows the velocities of (a) Helium (3.5 L/min) and (b) Argon (2.5 L/min) plasma jet as a function of axial distance along the jet's axis. It was noticed that, the bullet velocity increases with the increase in axial distance  $Z$  until reaches maximum value then it gradually decreases. The maximum plasma bullet velocity is  $8 \times 10^6$  cm/sec for Helium and  $4 \times 10^6$  cm/sec for argon.

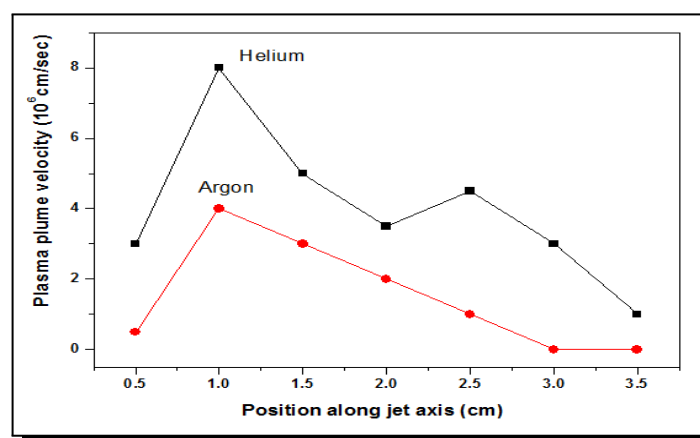


**Figure 9.** Plasma plume velocities along the jet axis for different gases (argon and helium) measured by using a dielectric probe

The decrease of bullet velocity with the increase in axial distance after maximum can be ascribed to the decrease of the kinetic energy of the charged particle and the increase of recombination rate due to the collision with atoms of surrounding air [12].

## 4. Conclusion

Simple configuration of an atmospheric pressure plasma jet with only a high-voltage electrode, placed in a plastic syringe, has been investigated. An atmospheric pressure plasma jets, having lengths of 2-4cm have been obtained. It was noted that the argon plasma formed filaments i.e. argon discharge worked in filamentary mode. On other hand helium plasma, the discharge was quite uniform without filaments. The geometry and the shape of the plasma jet were found dependent on the applied voltage and gas flow rate.

### Competing Interests

The author declares that he has no competing interests.

### Authors' Contributions

The author wrote, read and approved the final manuscript.

## References

- [1] N. Hardt and D. Koenig, Testing of insulating materials at high frequencies and high voltage based on the Tesla transformer principle, Conference Record of the *1998 IEEE International Symposium on Electrical Insulation*, Vol. 2, pp. 517 – 520 (1998), DOI: 10.1109/ELINSL.1998.694846.
- [2] B. T. Phung, T. R. Blackburn, R. Sheehy and R. E. James, Tesla transformer design and application in insulator testing, in *Seventh International Symposium on High Voltage Engineering*, Vol. 5, pp. 133 – 136 (1991).
- [3] G. C. Damstra and J. A. J. Pettinga, A six pulse kV Tesla transformer, Fifth International Symposium on High Voltage Engineering, Vol. 2, paper 62.13/1-3 (1987).
- [4] V. P. Gubanov, S. D. Korovin, I. V. Pegel, A. M. Roitman, V. V. Rostov and A. S. Stepchenko, Compact 1000 PPS High-Voltage nano-second pulse generator, *IEEE Transactions on Plasma Science*, **25**(2), 258 – 265 (1997), DOI: 10.1109/27.602497.
- [5] C. R. J. Hoffmann, A tesla transformer high-voltage generator, *Review of Scientific Instruments* **46**(1), pp. 1 – 4 (1975), DOI: 10.1063/1.1134057.
- [6] H. Matsuzawa and S. Suganomata, Design charts for Tesla-transformer-type relativistic electron beam generators, *Review of Scientific Instruments* **53**(5), 694 – 696 (1982), DOI: 10.1063/1.1137044.
- [7] G. A. Mesyats, V. G. Shpak, M. I. Yalandin and S. A. Shunailov, RADAN-EXPERT portable high-current accelerator, *Tenth IEEE International Pulsed Power Conference* **1**, 539 – 543 (1995), DOI: 10.1109/PPC.1995.596681.
- [8] R. Godfrey, E. R. Mathews, J. A. McDivitt and R. A. Petrone, Analysis of Apollo 12 lightning accident, NASA MSC-01540 (1970).
- [9] J. Bussey, Report of Atlas/Centaur-67/FLTSATCOM F-6 investigation board, Vol. 2, NASA (1987).
- [10] G. M. El-Aragi, Design, construction and optimization of tesla coil, *J. Phys Astron.* **5**(3) (2017), 123.

- [11] A. Begum, M. Laroussi and M. R. Pervez, Dielectric probe: a new electrical diagnostic tool for atmospheric pressure non-thermal plasma jet, *International Journal of Engineering & Technology* **11**(3) (2011), 209 – 215.
- [12] U. M. Rashed, Characterization of helium and argon atmospheric pressure cold plasma jet generated by DBD system, *Australian Journal of Basic and Applied Sciences* **10**(10) (2016), 209 – 216.
- [13] M. Laroussi, C. Tendero, X. Lu, S. Alla and W. L. Hynes, *Plasma Proc. Polym.* **3**, 470 (2006), DOI: 10.1002/ppap.200600005.
- [14] N. Barekzi and M. Laroussi, *Plasma Processes Polym.* **10**, 1039 (2013), DOI: 10.1002/ppap.201370036.
- [15] D. B. Graves, *J. Phys. D: Appl. Phys.* **45** (26), 263001 (2012), DOI: 10.1088/0022-3727/45/26/263001.
- [16] A. Shashurin, M. Keidar, S. Bronnikov, R. A. Jurjus and M. A. Stepp, *Appl. Phys. Lett.* **93**, 181501 (2008), DOI: 10.1063/1.3020223.
- [17] M. Keidar, A. Shashurin, O. Volotskova, M. A. Stepp, P. Srinivasan, A. Sandler and B. Trink, *Phys. Plasmas* **20**, 057101 (2013), DOI: 10.1063/1.4801516.
- [18] M. Laroussi, S. Mohades and N. Barekzi, *Biointerphases* **10**, 029401 (2015), DOI: 10.1116/1.4905666.